Journal of Multidisciplinary Engineering Science and Technology (JMEST)
ISSN: 2458-9403
Vol. 8 Issue 4, April - 2021

Numerical Analysis of Flameless Combustion in a Compact Chamber Burning Hydrous Ethanol

Bruna Oliveira Passos e Silva Siqueira[1]*, Marco. A. R. Nascimento[2], Lucilene de Oliveira Rodrigues[2], Cláudia Gonçalves de Azevedo[3], Christian Jeremi Coronado Rodriguez[2], Tulio Augusto Zucareli de Souza[2]

[1] Federal University of Lavras – UFLA, Engineering Department – DEG
Mailbox 3037, Aquenta Sol, Lavras, MG, CEP 37200-000
[2] Federal University of Itajubá – UNIFEI, Mechanical Engineering Institute – IEM
Av. BPS 1303, Itajubá, MG, CEP 37500-903, Brazil.
[3] Paulista State University Júlio de Mesquita Filho, Rosana Experimental Campus – UNESP
Av. of Barrageiros, 1881, Rosana, SP, CEP 19274-000, Brazil

***Abstract*— This paper presents the numerical simulation of a compact laboratory-scale combustion chamber designed to operate with flameless combustion technology, using hydrous ethanol as fuel. The purpose of the study is to validate the combustion modeling to perform a more in-depth analysis of the combustion atmosphere based on the temperature profiles, velocity fields and emissions of UHC, CO and NO to verify the development of the flameless combustion regime from burning liquid biofuels. In this paper, two different combustions models had their results of the numerical simulations analyzed: the *Eddy Dissipation Concept* (EDC) and the hybrid model *Finite Rate / Eddy Dissipation* (FRED). The temperature profiles and UHC, CO and NO concentrations obtained in the numerical simulations showed good agreement with the experimental results for the combustion modeling by the FRED model, with maximum deviations between 1.0 and 12.5% between the numerical and experimental temperature profiles and maximum deviations of 6% for the UHC, CO and NO numerical and experimental emission rates, allowing the validation of the developed numerical procedure. The EDC model hasn't satisfactorily reproduced the turbulent and chemical interactions of the combustion reactions that occur in the flameless of hydrous ethanol, significantly affecting the temperature distribution in the combustion atmosphere which presented maximum deviations of the order of 25% in relation to the experimental results. The validation of the combustion modeling by the FRED model allowed a global analysis of the combustion atmosphere and the numerical results revealed that during the experiment the combustion chamber used in the present study didn't operate in the flameless regime, but in the transition regime between conventional combustion and the flameless combustion regime. The numerical analysis showed that a longer operation time of the experimental combustion system is necessary for the development of the flameless.**

Keywords*— Flameless, Liquid Biofuel, Emissions, Computational Fluid Dynamic, Eddy Dissipation Concept, Finite Rate / Eddy Dissipation.

I. INTRODUCTION

In order to improve the efficiency of combustion processes and to reduce the emission levels of pollutants resulting from these processes, flameless combustion technology has attracted the attention of researchers both in the industrial environment and in the scientific community. The flameless combustion technology was initially developed with the objective of suppressing the thermal formation of NO_x in burners for heating industrial ovens using preheated combustion air. To achieve the flameless combustion regime a technique is used where hot gases from the combustion are recirculated within the combustion chamber at high speeds which results from the high momentum in the injection of the reagent promoting a progressive dilution of these and inert products of combustion raising the temperature of the combustor to higher levels to the autoignition temperature of the reaction mixture. Thus, it generates a well distributed reaction zone at relatively low temperatures and low oxygen concentrations leading to inhibition of the production of pollutants such as NO_x, mainly by the thermal mechanism [1].

Another important point that has been highlighted in research is the association between flameless combustion technology and liquid biofuels, since they have higher energy density than gaseous fuels. Biofuels have taken on an important role as a sustainable energy source and their burning through flameless combustion technology has shown a significant reduction in the pollutant emissions levels and high efficiency in energy generation, making these fuels a good alternative to replace fossil fuels in processes involving combustion [2].

There are some important parameters to ensure the formation of the flameless combustion regime, which are: the flow composition to the combustor inlet,

i.e., the concentration of fuel, air and hot gases of combustion, pressure and minimum residence time of the reagents, because they determine the auto ignition temperature of the mixture [1]. Some studies have emphasized the influence of the use of preheating the combustion air to ensure that the reaction mixture reaches the autoignition temperature to produce a well-distributed reaction zone and also in order to avoid the formation of thermal NO_x, but it was not assured that this parameter is a prerequisite for the flameless combustion regime, taking into account the results presented in some studies as [3] to [9], where the autoignition temperature of the mixture was achieved without preheating the combustion air.

Several experimental and numerical works available in the literature provide a consolidated base of concepts for the flameless combustion of gaseous fuels addressing the physical, chemical and thermodynamic characteristics of the process and its influence on the NO_x formation process. Abuelnuor et al. [10] presented a study on the characterization of a combustor that operates with flameless combustion technology with low NO_x emissions. A more recent application focused on renewable fuels was presented by [11], where the authors compare the efficiency of using biogas produced by the anaerobic digestion of biomass and organic wastes by micro-organisms compared to conventional fuels such as natural gas. Through numerical simulations it was observed that there is no need to add a lot of hydrogen to maintain the flameless combustion of biogas for the diluted oxidant flow. In addition, the flameless combustion mode is easily achieved by applying oxy-fuel.

As previously discussed, research involving gaseous fuels is at an advanced stage, while studies involving the flameless combustion of liquid biofuels are in the initial stage of research due to the particularities in the development of burners to operate in this combustion regime that involve aspects such as atomization, dispersion and vaporization of the fuel and its mixture with oxidizing gases [12] [13].

The first investigations on the flameless combustion of biofuels were carried out with fuels derived from carbonated biomass at the Kaneko Laboratory at the University of Tokyo. The experiments were performed in the combustor of a gas microturbine, previously preheated by gases resulting from conventional combustion at an earlier stage, which led to the development of the flameless combustion regime achieving low emission levels [2]. Subsequently, Cameretti et al. [14] developed new studies for the same combustor using bioethanol and kerosene as fuels and they observed that bioethanol flameless combustion has efficiency similar to the conventional kerosene efficiency combustion for the same air/ fuel ratio and the emission standard were close to zero. However, these analyses were done through numerical simulations in CFD and were not validated.

Yang et al. [15] modeled the flameless for burning liquefied propane gas. The models FRCM and EDC found in CFD were combined to predict the performance of the combustor for this new combustion technology. The numerical results for NO_x and CO compared to the experimental showed good agreement. The authors further showed that the temperature gradients are low and a homogeneous distribution of the flame throughout the combustion chamber concluding at the end that the combination of the two models mentioned above satisfactorily reproduced the flameless combustion regime.

Some numerical works about the modeling of flameless burning liquid fuels are also highlighted in the literature focusing on the influence of the spray characteristics generated in the formation of flameless combustion system. Torresi et al. [16] designed an aerodynamically staged swirled burner using the diesel as the fuel. The burner has been experimentally tested and numerically simulated under diluted and highly preheated inlet flow conditions. The author noted in the results that there was complete combustion of diesel oil, and also a practically uniform distribution of temperature field in the combustion atmosphere, showing that the purpose of reproducing the flameless combustion was achieved.

Jamali [17] simulated numerically the flameless combustion of turbulent sprays for ethanol generated from a swirl injector. The simulations were developed in ANSYS FLUENT. The turbulence models used were the standard k-ε, realizable k-ε and RSM modeling. For the combustion models the steady flamelet model and FGM (Flamelet Generated Manifold) were chosen. The results showed that the turbulence models standard k-ε, realizable k-ε were more suitable for the study, while an analysis of the concentration of OH (hydroxyl) radicals in the combustion atmosphere showed that the modeling of combustion through the FGM reproduced correctly two combustion zones with homogeneous distribution of OH radicals. Furthermore, their low concentration showed that there was no formation of concentrated flames along the combustion chamber characterizing the flameless combustion.

Some studies in the literature approach the use of EDC combustion models and the FRED model, which takes into account the concept of EDC modeling with the effects of finite-rate chemistry, for applications involving the flameless combustion. Aminian et al. [18] presented a comparison between these two combustion models in CH_4/H_2 jet-in-hot and diluted coflow flames in flameless conditions. The results showed that the prediction of extinction threshold in flameless conditions is attainable only through the application of the extended FRED extinction model on a well-resolved turbulence-chemistry interaction field and showed that model is able to describe many features of localized flame extinction under flameless condition. As for the standard EDC modeling, the authors concluded that the model requires further

testing and refinements to verify its applicability for modeling combustion systems in flameless conditions.

Bösenhofer et al. [19] presented an analysis for the different treatments for the structures of fine energy scales in reactive flows using the EDC model, where they showed that for the operation of combustion systems under the conditions of the flameless combustion regime it is necessary to adjust the constants related to the scales turbulent flow and temporal scales of the flow, but the constant adjustment only works for specific cases and should not be done randomly.

According to [20] to [22], the flameless combustion regime presents well-distributed reaction zones and low reaction rates due to the high dilution of oxygen resulting from the high rates of combustion gas recirculation in the reactive atmosphere. Thus, the use of the FRED model adds to the EDC model the extended concept of the effects of finite-rate chemistry, which responds better to the reaction rates that develop in flameless combustion.

The flameless combustion is a difficult regime to model numerically, because it involves high levels of dilution and temperature and chemical reaction rate relatively low, which requires careful modeling of the interaction between turbulence, combustion and chemistry of the process.

An overview of the works previously mentioned shows that research involving flameless combustion of liquid fuel is still under development. Xing et al. [2] highlight in their review of flameless liquid fuels that current experimental approaches are not sufficiently adequate for surveying distributions of pressure, temperature and rate of gas recirculation inside combustion chambers. The authors also emphasize that CFD modeling also needs to be improved, justifying the development of numerical procedures that adequately represent the flameless characteristics of liquid fuels so that the numerical simulations are totally reliable.

TABLE 1 presents relevant studies found in the literature on flameless combustion for various types of liquid and gaseous fuels that use the experimental and CFD approaches to analyze this combustion regime. In general, these studies evaluate the temperature field and the emission levels in combustors that operate in the flameless regime and provide a good basis for the development of the present work. Moreover, it is possible to observe in TABLE 1, that numerical studies in CFD on the flameless regime of liquid biofuels in compact combustion systems are still not expressive, creating new possibilities for further research in this line, such as the one present in this work.

Thus, this study aims to validate combustion modeling for numerical simulation in CFD of flameless combustion of liquid biofuels and to characterize the global combustion atmosphere through temperature profiles, velocity fields and UHC, CO and NO emission levels in order to promote a better understanding of this combustion technology from a physical and thermodynamic point of view when associated with the use of liquid biofuels.

After validation of the numerical modeling, it will be possible to evaluate the development of the flameless combustion regime from the numerical results in comparison with the experimental results of [12] thus raising a series of conclusions on the operation of the experimental combustion system to guarantee the occurrence of flameless.

The numerical procedure consists on evaluating the performance of the EDC and FRED combustion models in the representation of the flameless combustion of hydrous ethanol that occurs in a compact combustion chamber with a laboratory scale of 2 kW of power. The numerical simulations were performed using the commercial software ANSYS® CFX®, based on the finite volume method. Moreover, for the combustion of hydrous ethanol this study has considered the chemical reactions based on the global reaction mechanism with 70 elementary reactions and 26 major chemical species for ethanol / air reaction proposed were also considered by [23]. The validation of the numerical results was performed based on the experimental work of [12], where it has been compared the temperature distributions and species concentrations in predefined regions in the combustion chamber.

At the end of this study, the aim is to obtain information that allows the modeling of flameless hydrous ethanol and, in the future, of other liquid biofuels for application in small-scale combustion chambers for energy microgeneration. Besides, it aims for the replacement of existing fuels in the combustion systems, such as gas turbine combustors, and the design of new, highly efficient, compact combustion chambers with reduced levels of pollutant emissions.

II. Experimental Setup

The experimental test was developed by [12] in a compact combustion system in order to operate in the flameless combustion regime for burning hydrous ethanol injected from a flow blurry injector. In Fig. 1 the details of the combustion chamber and the flow blurry injector used for fuel injection are presented. The combustion chamber was built in stainless steel and has an internal diameter of 101 mm and a length of 330 mm, with a ceramic glass window that shows the interior of the chamber during combustion tests.

The fuel is injected into the chamber by the flow-blurry injector, located in a prechamber Fig. 1 as “Fuel”. The combustion air is injected into the chamber from eight holes concentric to the fuel injector, defined in Fig. 1 by “Combustion Air”. The combustion air is preheated before entering the combustion chamber through hot gases recovered from the combustion process.

The combustion process is started in the system through an ignition spark of the airfuel mixture in order to obtain a stable flame with rich combustion conditions. After this initial procedure, the chamber keeps operating in the conventional combustion regime for 1 hour and 40 minutes in order to preheat the combustion atmosphere and reach the ideal conditions for the operation of the chamber in the flameless combustion regime. Flue-gas composition data (CO2, UHC, CO, and NOx) were withdrawn at the exhaust duct using an iso-kinetic, water-cooled stainless steel probe. Temperature measurements were made with type K mineral insulated thermocouples (diameter 1.5 mm), with maximum measured temperature range of 1300 °C (accuracy ±0.1%). Continuous measurements of the sample gas composition and temperatures were carried out during tests [12].

TABLE 1 – STUDIES REVIEW OF FLAMELESS COMBUSTION OF LIQUID AND GASEOUS FUELS.

Authors	Fuel	Aproach	Description
Derudi et al. [3]	Liquid hydrocarbons	Experimental	This study is focused on the investigation of the sustainability of mild combustion for liquid hydrocarbons using a dualnozzle laboratory-scale burner.
de Azevedo et al. [12]	Ethanol	Experimental	This study describes a flameless biofuel combustion system for burning hydrous ethanol, atomized by a blurry injector. The flameless regime was characterized by measurements of spatial distributions of temperatures and flue-gas composition.
Castela et al. [6]	Natural gas	Experimental	Evaluation of the combustion regimes occurring in a small-scale laboratory cylindrical combustor burning natural gas.
Kumar at al. [33]	Liquified Propane Gas	Experimental and CFD	Optimization of the geometry of a 3 kW laboratory combustion using numerical simulation and experimental procedure.
Cameretti et al. [14]	Bioethanol and Kerosene	CFD	Numerical simulation in CFD in gas microturbine combustion to analyze the flameless combustion regime through the temperature profiles and emission levels that is developed in the combustion.
Torresi et al. [16]	Diesel	Experimental and CFD	An aerodynamically staged swirled burner fuelled by diesel oil has been experimentally tested and numerically simulated under diluted and highly preheated inlet flow conditions, in order to analyze the burner performance operating in the flameless regime.
Jamali [17]	Ethanol	CFD	It simulated numerically the flameless combustion of turbulent sprays for ethanol generated from a swirl injector. The turbulence models used were the standard k-ε, realizable k-ε and RSM modeling. For combustion models the steady flamelet model and FGM (Flamelet Generated Manifold) were chosen.
Aminian et al. [18]	CH_4/H_2	CFD	This study presents a comparison between the EDC and FRED combustion models in the modeling of CH4/H2 jet-in-hot and diluted coflow flames in flameless conditions.
Bösenhofer et al. [19]	-	CFD	This study presents an analysis of the different treatments for the structures of fine energy scales in reactive flows using EDC modeling.
Present paper	Hydrous Ethanol	CFD	This study validates a numerical procedure for simulating the flameless combustion regime in a compact 2 kW combustor in order to verify the development of the flameless combustion regime from a global analysis of thermodynamic and physical parameters that occur in the combustion atmosphere for burning liquid biofuels.

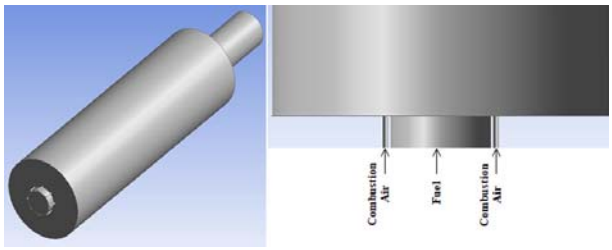

Fig. 1 - Details of the compact combustion system used in the numerical simulations based in geometry used in experiments of de Azevedo [12].

III. MATHEMATICAL MODELING AND METHODOLOGY

Numerical simulations of flameless combustion of hydrous ethanol were performed using the CFD ANSYS CFX tool. Among the models available in this numerical tool, the turbulence model RNG k-ε was selected, which presents high performance in reactive flow modeling. The heat transfer was modeled by the Discret Transfer model and the flow of particles was modeled by the Discret Phase Model. In order to represent the chemical kinetics of the combustion reactions of hydrous ethanol, the global reaction mechanism was used with 70 elementary reactions and 26 major chemical species for ethanol/air reaction proposed by [23]. To represent the flow inside the combustion chamber, an Euler/Lagrange approximation was used to describe the two-phase gas-liquid flow. The walls that represent the computational domain are treated with the standard wall function recommended by [24].

For combustion modeling, two available models in ANSYS CFX were considered, the EDC and the FRED, in order to select the best model for representing the flameless combustion of liquid biofuels, in the procedure developed in the present work. The combinations between models for performing numerical simulations and the development of the modeling procedure are represented in the TABLE 2.

TABLE 2 – MODELS USED IN NUMERICAL SIMULATIONS.

	Turbulence model	Combustion model	Radiation model
Modeling 1	RNG k-ε	EDC	Discret Transfer
Modeling 2	RNG k-ε	EDC/FRC	Discret Transfer

A. *Turbulence Model*

In the RNG k-ε turbulence model, the equations of the standard k-ε model are derived applying a statistical technique to the instant Navier-Stokes equations, resulting in new equation including a term in ε equation for the interaction between turbulent dissipation and the average shear, an analytical formula for the number of turbulent Prandtl and a differential formula for the effective viscosity, which allows a deeper analysis of the effects of the vorticity in turbulence.

In this model, turbulent kinetic energy, k, is defined as a variation in velocity fluctuations and ε is turbulent dissipation, being the rate at which velocity fluctuations dissipate.

The choice of the RNG k-ε model was made based on the studies presented in [17] and [25], where it was observed that the present model promotes a better turbulent interaction between the liquid and gaseous phases in the flow, better mixing of the reagents in the combustion process and higher rate of flue gas recirculation favoring the formation of an almost homogeneous combustion atmosphere.

B. *Combustion Models*

1) Eddy Dissipation Concept Model (EDC)

The EDC model provides an empirical expression for the mean reaction rate based on the assumption that chemical reaction occurs in the regions where the dissipation of turbulence energy takes place. In flows of moderate to intensive turbulence, these areas are concentrated in isolated regions, occupying only a small fraction of the flow. These regions consist of “fine structures” whose characteristic dimensions are of the order of Kolmogorov’s length scale in two dimensions. The fine structures are not evenly distributed in time and space [26].

2) Finite Rate / Eddy Dissipation Combustion Model (FRED)

The combustion model FRED combines the concepts of models Eddy Dissipation Concept (EDC) and Finite Rate Chemistry (FRCM). Eddy Dissipation Concept model assumes that for turbulent flow, chemical reactions occur only if the reactants are mixed at the molecular level with the smaller scales, i.e., turbulent kinetic energy contained in large flow structure is transferred to the fine structures in which this energy it is dissipated as heat. These fine structures are small vortices in the Kolmogorov scale and are responsible for mixing at the molecular level, which can be modeled as a well-mixed reactor. The dissipative fine structures are distributed intermittently along the flow causing only part of these can be burned [27]. The Finite Rate Chemistry Model shows that the effects of turbulent fluctuations can be neglected and reaction rates are determined by Arrhenius kinetic expression. Thus, the methodology applied in the combined model FRED consists in calculating the reaction rate for both models separately with the respective formulations, and the minimum value obtained between the two is used. This calculation occurs on every step of the reaction, since the model should take into consideration if the reaction is limited by the chemical kinetics or by the turbulent interaction every time step of the reaction and for each physical location in the combustion atmosphere.

C. *Discret Transfer Radiation Model*

This model is based on tracing the domain by multiple rays leaving from the bounding surfaces. The technique was developed by [28] and depends upon the discretization of the equation of transfer along

rays. The path along a ray is discretized by using the sections formed from breaking the path at element boundaries. The physical quantities in each element are assumed to be uniform.

D. *Spray Modeling*

The fuel injection in the combustion chamber simulated in the present work is performed from a flow blurry injector. The spray produced has a dispersion of cone shaped drops, the entire area of which is occupied by drops of hydrous ethanol.

The spray modeling is performed using DPM that follows an Eulerian-Lagrangian approach where the fluid and gas phase flow is treated as a continuous medium and the solution is realized through the Navier-Stokes equations and the dispersed phase (gas bubbles, droplets or solid particles) is represented by a large number of particles having their trajectories calculated according to the Lagrangian reference, where the trajectories of the particles are calculated individually for specific time intervals. Following this concept, the cone with the primary drop model was chosen for modeling the ethanol spray, assuming values for mass fuel rate, spray cone angle, the number of injected particles within the domain and air velocity that assists in the dispersion fuel in the form of drops.

An important phenomenon that should be considered in this modeling step is the fuel evaporation, which aims at modeling the evaporation of a liquid species into particles for the respective species in the gas phase, so that these interact with the continuous phase and ensure the development of the combustion reactions. Furthermore, the modeling of evaporation of ethanol drops, the size of the drop and the drop in temperature that occurs in the formation of the fuel spray are governed by the mass and heat transfer during the fuel evaporation process [29]. Thus, the evaporation of ethanol drops was modeled by Liquid Evaporating Model available in ANSYS CFX.

I. Domain and Boundary Conditions

A. *Boundary conditions*

The details of the initial boundary conditions used to perform the numerical simulations are presented in the TABLE 3. The combustion air is injected into the combustion chamber at a speed of 47.35 (m/s) through eight holes concentric to the fuel spray injection region and the excess air coefficient, λ, is equal to 1.65. The fuel spray, produced by a flow-blurry injector, has a cone angle equal to 21° and a mass flow rate of 0.08 (g/s). The regions where the boundary conditions are considered are shown in the Fig. 2. Fig. 2.A shows the combustion air inlet region, which is defined by the velocity inlet boundary condition, $V_{combustion\_air}$ (see Table 3). Fig. 2.B shows the spray injection region, which is represented by the arrow cone, denoted by *Spray cone angle* in Table 3. In the Fig. 2.C the exhaust region of the flue gases is shown at the bottom left, whose boundary condition is defined as ***Outlet***.

As provided in [30], the process of atomization of liquid fuels is not well understood because of the difficulty of access to the denser region of the spray both numerical and experimental way. Thus, most of the simulations are initialized with the already atomized spray and droplets with a distribution defined by experimental tests of [31] and [32].

TABLE 3 – BOUNDARY CONDITIONS USED IN NUMERICAL SIMULATIONS.

Boundary Conditions	
λ	1.65
$V_{combustion\_air}$	47.35 (m/s)
$\dot{m}_{fuel}$	0.08 (g/s)
Spray cone angle	21°
Power	2 (kW)

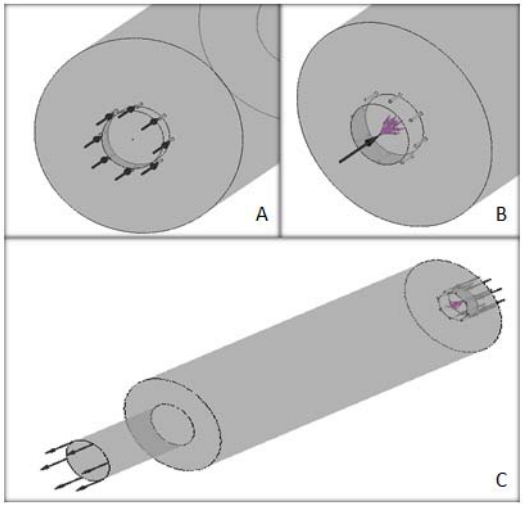

Fig. 2 – *Combustion chamber regions where the initial boundary conditions are defined: (A) Combustion air inlet; (B) Spray injection region and (C) Flue gas exhaustion.*

B. *Numerical mesh*

To choose the mesh, mesh independence tests were performed for the boundary conditions defined in TABLE 4. The tests were carried out considering three unstructured meshes, with different degrees of refinement and for the definition of the best mesh, the average numerical and experimental temperature gradient (ΔT_{mean}) values were compared.

The meshes used are shown in TABLE 4, with their respective element numbers.

TABLE 4 – MESH INDEPENDENCE TEST RESULTS.

Mesh	Number of Elements	$\Delta T_{mean\_experimental}$ (°C)	$\Delta T_{mean\_numeric}$ (°C)	Deviation (%)
01	310,618	230.19	200.15	15.01
02	412,372		180.39	27.6
03	639,464		230.17	0.466

TABLE 4 shows that the numerical temperature gradients of meshes 01 and 02 showed a difference of

15.01% and 27.6% above the experimental value, while mesh 03 showed an error of 0.466% in concerning the experimental value. The high difference between the numerical and experimental temperature gradients obtained with meshes 01 and 02 are related to the low refinement of the chamber mesh, which does not allow a more precise numerical calculation of the chemical and thermodynamic phenomena that occur in the combustion atmosphere. Mesh 03 (see Fig. 3) presented a very low error between temperature gradients due to the greater degree of refinement, being chosen to perform the numerical simulations of the present article.

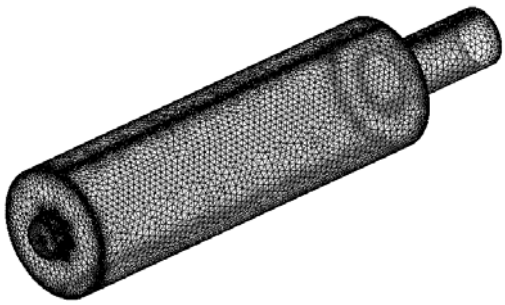

Fig. 3 – Representation of computational Mesh 03 used in numerical simulations.

V. Results and Discussion

In this topic, the results obtained in the numerical simulations with the model combinations defined in TABLE 2 are presented considering the initial boundary conditions presented in TABLE 3. The differences and comparisons for the performed models are based on the temperature profiles that are developed in the atmosphere combustion and the composition of the exhaust gases UHC, CO and NO. For validation of the modeling, the numerical results are compared to the experimental results of [12].

A. Temperature profiles

To obtain the axial numerical temperature profile inside the chamber, measurement points distributed in the combustion atmosphere were considered as indicated in the experimental measurement procedure of [12], in which six thermocouples were installed along the axial direction of the chamber 50, 140, 200, 260 and 280 mm away from the base of the chamber and, according to the stabilization of the combustion chamber operating conditions, average local temperatures were measured at radial direction at points 5, 15, 25, 35 and 45 mm, in relation to the combustion chamber wall. The temperature measurement mesh is shown in Fig. 4.

In the Fig.s between Fig. 5.A and Fig. 5.E it is presented the experimental temperature profiles and for the EDC model, for the measurement points indicated in Fig. 4.

In Fig. 5, it's possible to realize that the numerical temperature profiles do not show good agreement with the experimental results. At all radial measurement points from the center to the vicinity of the chamber wall (See Fig. 5.A to Fig. 5.E) the numerical temperature values do not vary significantly, showing that the entire combustion atmosphere is between 700 and 800 ° C, while the experimental result indicates values between 690 °C and 921 °C. It is still possible to notice that the average temperature values in each measurement position are underestimated by EDC modeling.

The numerical temperature profiles show a value, practically constant of temperature in the combustion atmosphere, with a temperature gradient of the order of 63.2 °C, a value that is very different when compared to the experimental temperature gradient that is equal to 230.2 °C.

Fig. 6 shows the temperature distribution in the combustion atmosphere in the analyzed chamber, where it can be observed that the temperature is constant throughout the combustion atmosphere. The numerical temperature profiles were affected by the inability of the EDC model to capture the chemical and turbulent interactions in the reaction zone of the problem under study. This model is widely used for modeling conventional combustion processes, where chemical reactions occur in small areas and these reactions are limited by mixing rates. In the case of flameless combustion, the opposite occurs, the reaction zones are homogeneously distributed in the combustion atmosphere and chemical reactions rates are slower due to the low concentrations of oxygen found in the reaction zones [19].

According to [16], the use of the EDC model is very common in simulations of the flameless combustion regime of fuels such as pulverized coal and gaseous fuels. However, there's a common problem in these simulations, which the temperature values in the combustion atmosphere are overestimated when using this model. In the numerical simulations of the present work, it appears that for the liquid biofuel used, the temperature values are with average values below the experimental temperatures, showing that the model does not respond satisfactorily in the analyzed condition.

The alternative measure for solving this problem is the modification of the speed, energy, turbulence and reaction constants in the EDC model in order to adjust them to the flameless combustion regime in order to improve the numerical results of temperature. Studies developed by [33] show the attempt to modify these constants to adapt to the modeling of the flameless combustion regime, although these changes were satisfactory only for some cases such as burning gaseous fuels for instance.

Based on previously cited work, the constants of the EDC model were not changed in the present work, as information on EDC modeling of flameless combustion of liquid fuels and biofuels available in the specialized literature on the subject is still obscure, which can lead to errors and confusing results in the numerical simulations for the study developed here.

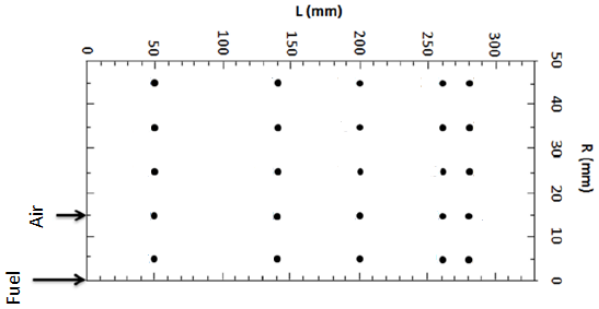

Fig. 4 – Mesh for temperature measurement in the combustion atmosphere (Reproduced from [12]).

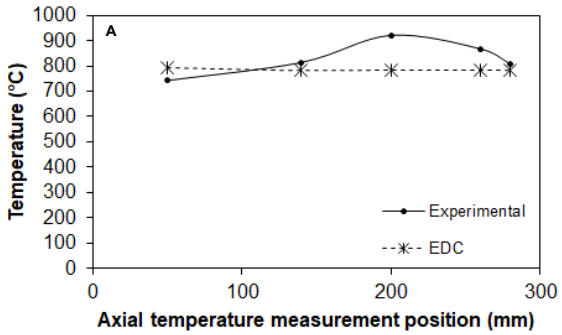

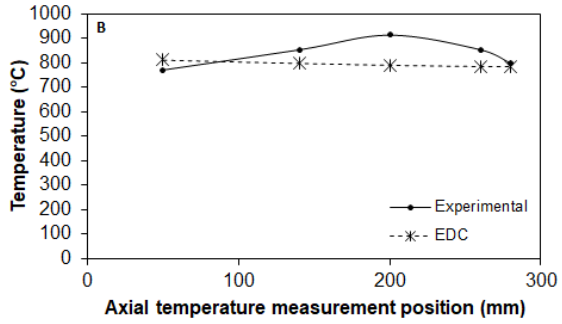

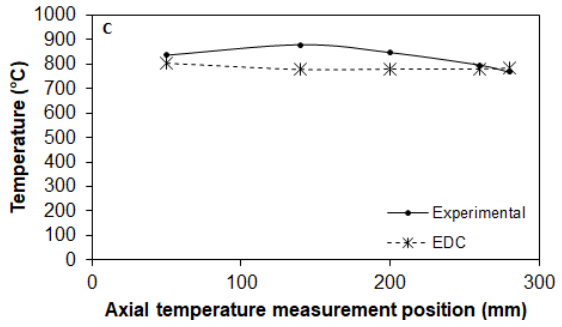

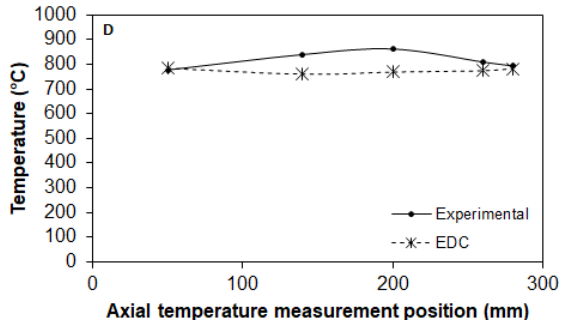

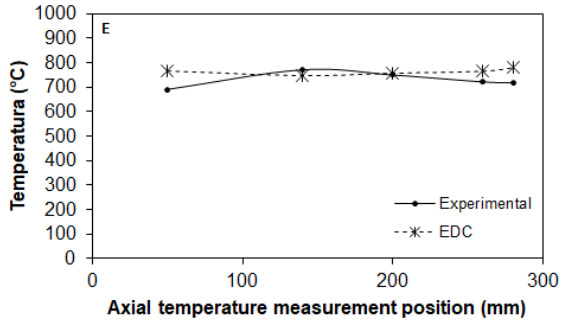

Fig. 5 – Temperature profile inside the chamber using the combustion model EDC, measuring: (A)45 mm, (B) 35 mm, (C) 25 mm, (D) 15 mm and (E) 5mm from the chamber's wall.

Fig. 6 shows the temperature distribution in the combustion atmosphere in the analyzed chamber, where it can be observed that the temperature is constant throughout the combustion atmosphere. The numerical temperature profiles were affected by the inability of the EDC model to capture the chemical and turbulent interactions in the reaction zone of the problem under study. This model is widely used for modeling conventional combustion processes, where chemical reactions occur in small areas and these reactions are limited by mixing rates. In the case of flameless combustion, the opposite occurs, the reaction zones are homogeneously distributed in the combustion atmosphere and chemical reactions rates are slower due to the low concentrations of oxygen found in the reaction zones [19].

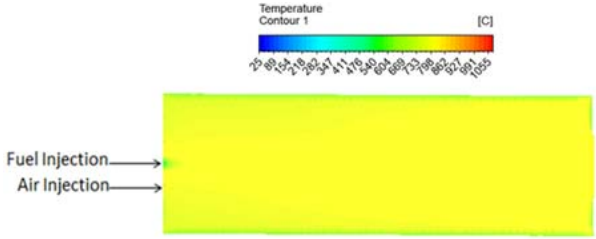

Fig. 6 – Temperature distribution in the median plane of the combustion chamber using the EDC combustion model.

According to [16], the use of the EDC model is very common in simulations of the flameless combustion regime of fuels such as pulverized coal and gaseous fuels. However, there's a common problem in these simulations, which the temperature values in the combustion atmosphere are overestimated when using this model. In the numerical simulations of the present work, it appears that for the liquid biofuel used, the temperature values are with average values below the experimental temperatures, showing that the model does not respond satisfactorily in the analyzed condition.

The alternative measure for solving this problem is the modification of the speed, energy, turbulence and reaction constants in the EDC model in order to adjust them to the flameless combustion regime in order to improve the numerical results of temperature. Studies developed by [33] show the attempt to modify these

constants to adapt to the modeling of the flameless combustion regime, although these changes were satisfactory only for some cases such as burning gaseous fuels for instance.

Based on previously cited work, the constants of the EDC model were not changed in the present work, as information on EDC modeling of flameless combustion of liquid fuels and biofuels available in the specialized literature on the subject is still obscure, which can lead to errors and confusing results in the numerical simulations for the study developed here.

The second combustion model used was the FRED model, since there has been a failure in regards of the combustion modeling by the EDC concept. The hybrid FRED model adapts well to reactive flows where turbulent interactions are high and reaction rates are low, as in the flameless combustion regime.

Fig. 7 shows the temperature profiles measured according to the measurement grid in Fig. 4, where it can be seen that the numerical temperature profiles show good agreement with the experimental temperature profiles of [12]. The average temperature found in the numerical simulation is of the order of 823.7 °C while the experimental value is 807.7 °C. The temperature numeric gradient is equal to 230.17 °C, a value that is very consistent with the experimental temperature gradient which is equal to 230.2 °C.

Still regarding temperature profiles, it can be observed for the numerical and experimental results that the highest temperatures are located in the vicinity of the central axis of the chamber, as observed in Fig. 7.A and Fig. 7.B, where the highest values of temperatures are above 900 °C. In Fig. 7.C to Fig. 7.E,, it is observed that as the approach to the chamber wall occurs, the temperature values begin to decrease, reaching values below 900 °C. This is due to the heat transfer by radiation and the decrease in the intensity of combustion reactions. This behavior of the temperature distribution in the combustion atmosphere is one of the intrinsic characteristics of the flameless combustion regime.

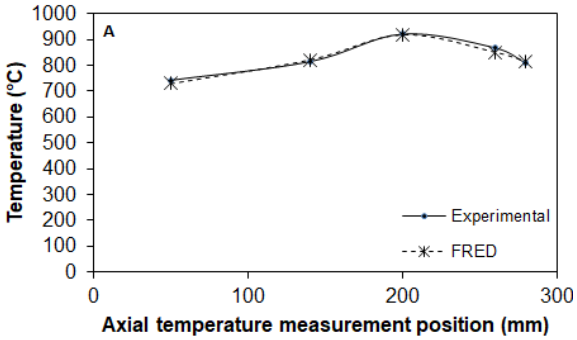

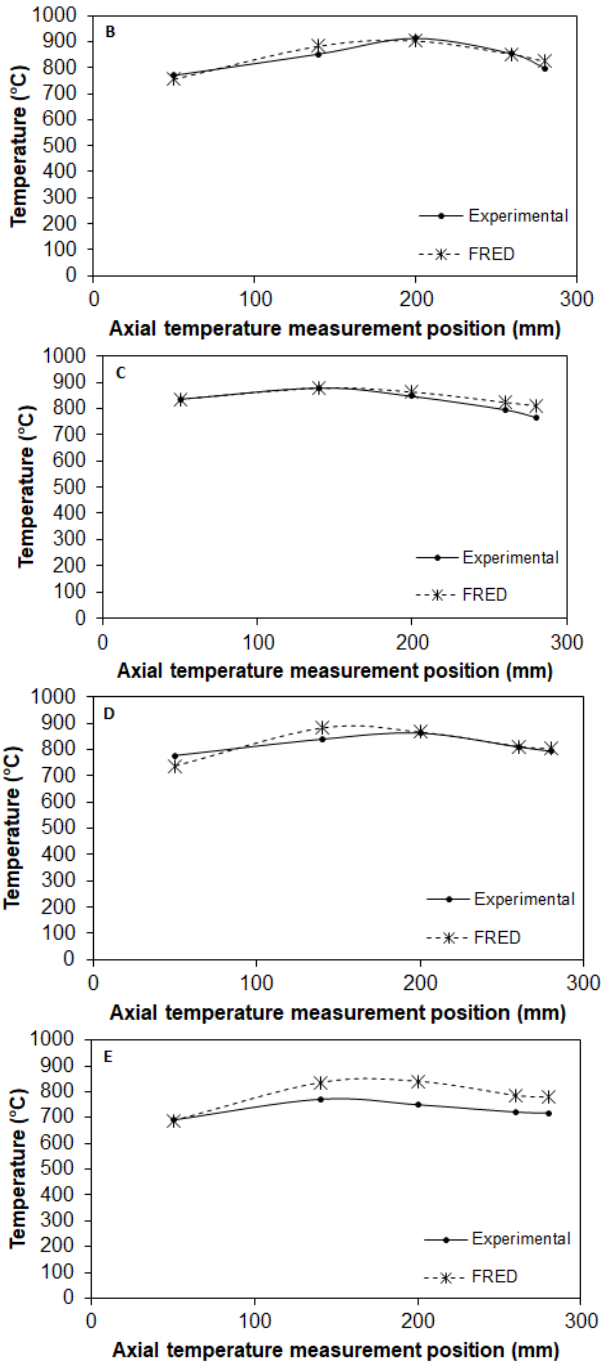

Fig. 7 – Temperature profile inside the chamber using the FRED combustion model, measuring: (A) 45 mm, (B) 35 mm, (C) 25 mm, (D) 15 mm e (E) 5mm from the chamber wall.

1) Flameless Combustion Considerations

In this item, a discussion will be presented about the flameless combustion regime from the temperature profiles obtained in the numerical simulations and the characterization of the combustion atmosphere.

The validation of the results of the numerical simulations using the FRED combustion model through the temperature profiles allowed a more in-depth analysis of the combustion atmosphere, given

that the simulations were developed through a three-dimensional geometry, leading to important conclusions about the combustion regime that develops inside the chamber.

Fig. 8 shows the spatial distribution of temperatures in the combustion atmosphere for the upper medium plane of the compact combustor under study in the present work. Fig. 8.A corresponds to the experimental work of [12] and Fig. 8.B corresponds to the numerical result obtained in this work for the FRED combustion model. The temperature profiles are considered for the region represented by the experimental measurement grid defined previously in Fig. 4. Comparing the temperature distribution in Fig. 8.A and Fig. 8.B, it can be seen that the maximum temperature values are concentrated in the regions close to the measuring points in the axial direction at positions 150 and 250 mm in both cases. The temperature increases along the axis of the chamber, until the moment when it reaches a maximum value that corresponds to the region where there is an effective mixture between the reagents and the recirculated combustion gases. The increase in temperature in the central region of the chamber corresponds to the temperature peaks observed in Fig. 7.A to Fig. 7.C, which characterizes a region of flame concentration.

Fig. 9 shows the complete combustion atmosphere in the middle plane of the chamber. It is possible to observe a gradual increase in temperature according to the temperature contours, with temperatures varying between 690 and 920 °C, according to the experimental results of [12]. However, the numerical temperature contours show that there is still a concentration of flame in the central region at the top of the combustion atmosphere, which is in accordance with the experimental temperature profile shown in Fig. 8.A. The same behavior is not observed in the lower half of the combustion atmosphere (see Fig. 9), where the temperature distribution is more homogeneous. This set of observations allows us to state that the combustion system is not yet fully operating in the flameless combustion regime, but in the transition from conventional combustion to the flameless regime, due to the presence of a flame concentration in the upper part of the medium plane of the atmosphere combustion, a fact reinforced by the temperature profiles presented previously in Fig. 7.

Some characteristics that reinforce that the system is transitioning to the flameless combustion regime are the absence of isolated hot spots in the combustion atmosphere, absence of a flame sustained in the vicinity of the injector and decreasing the temperature in the combustion atmosphere in the radial direction, with lower temperatures in the vicinity of the chamber wall (See Fig. 8.B).

As the numerical results led to the conclusion that the experimental combustion system is operating in the transition regime between conventional and flameless combustion, the hypothesis is raised that the combustion chamber's operating time was not enough to guarantee the development of the flameless in every combustion atmosphere. To verify this hypothesis, the numerical simulation time was increased from 550 numerical advances to 1000 numerical advances in time in order to analyze the behavior of the combustion system.

In Fig. 10, it can be seen that with a longer simulation time there was a better distribution of the flame. Comparing Fig. 9 and Fig. 10 in the upper middle plane of the combustion atmosphere, it is possible to notice that, in Fig. 10, there is no flame concentration and the temperature distribution is homogeneous in the combustion atmosphere, keeping in the range between 690 and 920 °C and with a temperature gradient of approximately 230 °C. There are also no hot spots in the combustion atmosphere and flame formation in the fuel injection region and the temperature profile is practically symmetrical when comparing the upper and lower middle planes of the combustion atmosphere.

Fig. 11 shows a comparison between the speed field between the numerical simulation with 550 numerical advances in time (see Fig. 11.A) and 1000 numerical advances in time (see Fig. 11.B). In Fig. 11.A it is observed that the flow develops with a higher speed range up to the region of approximately 300 mm in the axial direction of the chamber and in the upper middle plane of the combustion atmosphere, this flow promotes a greater drag of drops from the fuel for this region leading to the concentration of flame in that area of the combustion atmosphere, as observed in Fig. 9 .

It is also possible to verify in Fig. 11.A that the flow recirculation zone is concentrated in the central part of the chamber, which disadvantages a homogeneous distribution of the reactant mixture in the combustion atmosphere and, consequently, helps in the development of a flame concentrated in the upper middle plane of the combustion chamber.

In Fig. 11.B there is a change in the flow velocity field inside the chamber. It is observed that the recirculation zone between the reaction mixture and the gases resulting from the combustion reaches a more elongated region in the combustion atmosphere. This fact is the result of the better speed distribution that occurs due to the longer operation time of the combustion chamber. It is noted that the highest flow velocities reach approximately the 250 mm region in the axial direction of the chamber in the upper middle plane and in the lower middle plane of the chamber there is also a higher speed of recirculation favoring the mixing process between reagents and hot gases resulting from combustion and, consequently, favoring the development of a reaction zone better distributed in the combustion chamber and a uniform temperature distribution in the combustion atmosphere, as previously observed in Fig. 10.

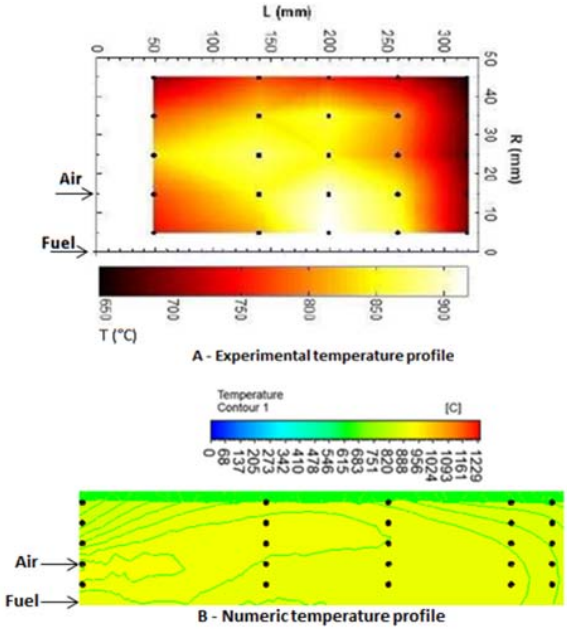

Fig. 8 – Comparison between the spatial temperature distribution: (A) experimental result [12] and (B) numeric result.

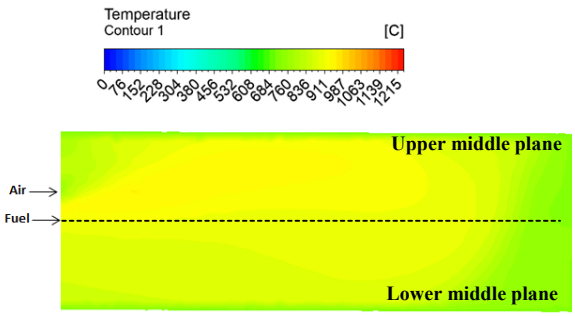

Fig. 9 – Complete combustion atmosphere in the middle plane of the chamber for 550 numerical advances in computational time.

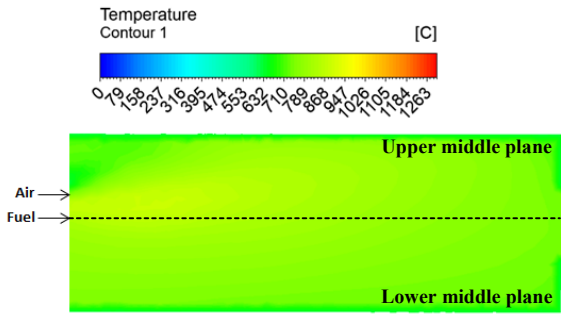

Fig. 10 – Complete combustion atmosphere in the middle plane of the chamber for 1000 numerical advances in computational time.

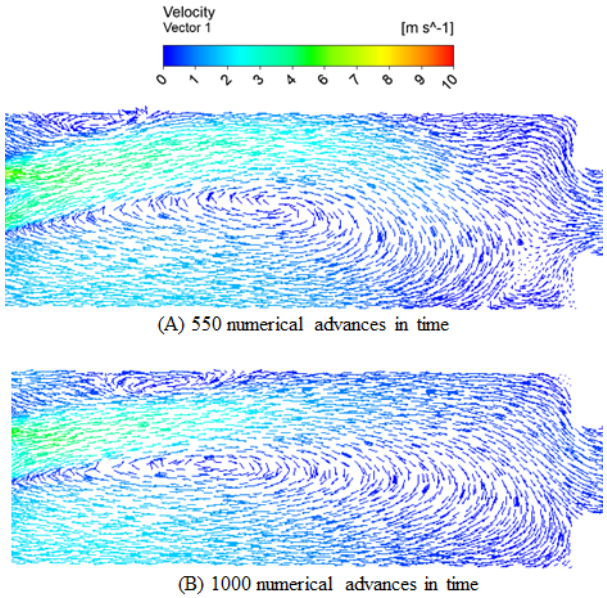

Fig. 11 – Velocity distribution inside the combustion chamber.

With these results it is possible to conclude that the increase in the simulation time improved the conditions of the reactive flow inside the chamber, for example, a better mixture between the reagents and the recirculation gases resulting from the combustion and an improvement in the recirculation rate of the hot gases combustion, which promotes a homogeneously distributed reaction zone, implying greater uniformity in the distribution of temperatures in the combustion atmosphere. These characteristics confirm the development of the flameless combustion regime with the increase of the combustion chamber operating time.

A general analysis of the results obtained through the numerical procedure developed in the present work shows that the experimental procedure can be optimized from the point of view of the system's operating time, since the experimental results obtained by [12] show the transition of the combustion regime conventional for the flameless combustion regime, that is, after reaching the transition regime, it is necessary for the system to operate for some time so that there are more suitable conditions for the development of the flameless combustion regime as shown in Fig. 10 and Fig. 11.B for the numerical simulation with 1000 numerical advances in time.

B. Composition of Exhaust Gases

One of the main characteristics of the flameless combustion regime is the reduction of NO_x, UHC and CO emissions. Therefore, an analysis of the emissions of these three types of gases was carried out in order to investigate the efficiency of the reaction mechanism for hydrous ethanol from [23] in the representation of the burning of this fuel by the flameless combustion regime using the FRED combustion model.

As the temperature profiles did not show good agreement with the experimental results of [12], the EDC combustion model was not considered in the analysis of emissions. This difference between the numerical and experimental temperature fields shows that this model does not correctly represent the chemical/turbulent interactions that occur in the combustion atmosphere and this affects the concentration of species present in the exhaust gases of the combustion process under study.

For this stage of the validation, numerical simulations were carried out, varying the excess air coefficient, λ, in the combustion process, according to the experimental work of [12] and at the end the numerical and experimental UHC, CO and NO emission rates were compared.

Fig. 12 to Fig. 14 show the emissions of UHC, CO e NO, respectively, as a function of λ, operating in the flameless combustion regime at power of 2 kW. The values of the emission levels as a function of λ are shown in TABLE 5. It is possible to observe that there is a good agreement between the numerical and experimental results for emissions, which were extremely low for operating conditions (See TABLE 5). The increase in λ promoted a decrease in CO and UHC. This happens because the increase of λ that results in an increase of the combustion air inlet velocity, which increases the rate of recirculation of the hot combustion gases in the chamber, promoting a good mixing between the reactants and the inert gases of combustion, causing a decrease in the concentration of UHC and CO (see Fig. 12 and Fig. 13) in the exhaustion system.

The increase in the rate of recirculation of the hot combustion gases also promotes a decrease in the global temperature in the combustion atmosphere improving the dilution of O_2 significantly in this region. Thus, the CO oxidation reactions are inhibited, causing a dramatic drop in emissions of CO (see Fig. 13).

NO levels for the numerical simulations remained below 3.5 ppm for operating conditions (see Fig. 14). An explanation for this fact is the almost uniform temperature distribution in the combustion atmosphere, which presents low values, causing a reduction in NO formation. The increase of λ also influences the reduction of NO formation due to the greater dilution of the reaction mixture.

In this study there is no set the primary NO formation mechanism, because the reactions for NO are inserted directly into the reaction mechanism used in the simulations. Based on the temperature values it can be concluded that the most NO is formed from the immediate mechanism (prompt NO) and N_2O mechanism.

Mancini et al. [34] shows in their study that immediate mechanism is responsible for the formation of only 5% of NO, while the remainder is formed by the N_2O mechanism, the latter being very important in combustion systems that work at low temperatures to inhibit the formation of thermal NO [14].

For CO emissions there is a considerable difference in numerical and experimental CO concentrations for λ = 1.65 (See Fig. 13). Based on the proximity of the emission values for NO and UHC elements, it can be said that a problem has occurred at the time of experimental measurement of the CO level for the respective λ values, which may be associated with failure of the measuring equipment or instabilities in the combustion system at the time of data acquisition.

The maximum deviation between the numerical and experimental UHC, CO and NO concentration values was approximately 6.0%. Hence, it can be said that the reaction mechanism of Verma [23] represents satisfactorily the reactions that are developed during the burning of hydrous ethanol in the flameless combustion regime for the combustion modeling by the FRED concept.

The emission results presented in Fig. 12 to Fig. 14 were obtained for the numerical simulation performed with 550 advances in time. In order to analyze the influence of the time of operation of the compact combustion system to obtain the flameless combustion regime in the emissions of the system, a discussion will be held taking into account the numerical simulation with 1000 advances in time.

TABLE 5 – NUMERIC AND EXPERIMENTAL EMISSION LEVELS OF UHC, CO AND NO ACCORDING TO λ FOR THE FRED COMBUSTION MODEL.

λ	**1,65**		**2.05**	
	Numeric	Experimental	Numeric	Experimental
UHC (ppm)	1.404	1.427	1.141	1.075
CO (ppm)	3.270	14.216	3.880	3.719
NO (ppm)	3.200	3.078	2.677	2.774
λ	**2.26**		**2.45**	
	Numeric	Experimental	Numeric	Experimental
UHC (ppm)	1.030	1.010	1.052	1.010
CO (ppm)	3.152	3.334	3.199	3.229
NO (ppm)	2.521	2.649	2.396	2.555

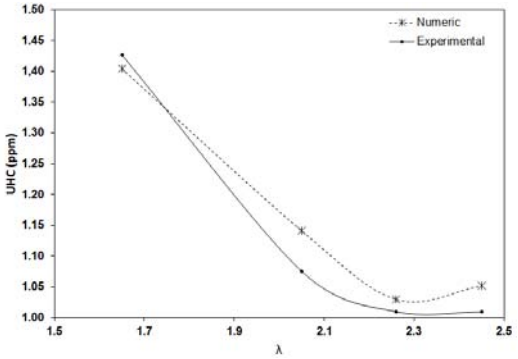

Fig. 12 – Comparison between numerical and experimental UHC emission levels.

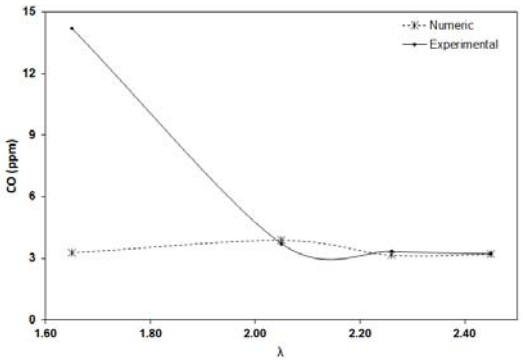

Fig. 13 – Comparison between numerical and experimental CO emission levels.

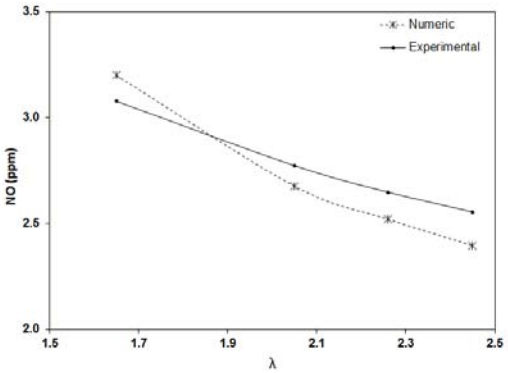

Fig. 14 – Comparison between numerical and experimental NO emission levels.

TABLE 6 shows the emission rates of UHC, CO and NO obtained in the numerical simulations with 550 and 1000 numerical advances in time. The comparison between the numerical results shows that there was a decrease of approximately 10% in the values of the emission levels of NO, UHC and CO for the simulation with 1000 numerical advances. The decrease in values was not so significant because even though there was a better distribution of temperatures in the chamber, the temperature values in the combustion process did not undergo major changes. But what is concluded from this result is that the emission rates of UHC, CO and NO decrease as soon as the combustor starts operating in the flameless regime, due to the better mixing conditions between the reactants and the hot combustion gases, which result in a homogeneous distribution of the reactions in the combustion atmosphere, providing greater efficiency in burning the reaction mixture.

TABLE 6 – POLLUTANT EMISSION VALUES FOR NUMERICAL SIMULATIONS WITH 550 AND 1000 NUMERICAL ADVANCES OVER TIME.

Simulation with 550 numerical advances			
λ	NO (ppm)	UHC (ppm)	CO (ppm)
1.65	3.200	1.404	3.270
2.05	2.677	1.141	3.880
2.26	2.521	1.030	3.152
2.45	2.396	1.052	3.199
Simulation with 1000 numerical advances			
λ	NO (ppm)	UHC (ppm)	CO (ppm)
1.65	2.880	1.268	2.952
2.05	2.510	1.033	3.493
2.26	2.270	0.932	2.838
2.45	2.152	0.947	2.883

VI. CONCLUSIONS

In the present work it was presented the validation of a procedure for the realization of a 3D numerical simulation of flameless combustion of hydrous ethanol in a compact combustion chamber of 2 kW to carry out a thorough analysis of the combustion atmosphere from the physical and thermodynamic point of view to characterize the flameless combustion regime using liquid biofuel. The ANSYS CFX computational fluid dynamics software was used for numerical modeling.

The first analysis of results was related to the temperature profiles obtained in the numerical simulations. The numerical temperature profiles using the EDC combustion model did not show good agreement with the experimental results of [12]. For this modeling, the temperature values were underestimated, presenting values between 700 and 800 °C, with errors above 25% in comparison with experimental values found in the 690 to 921 °C. Due to the discrepant difference between the temperature values, the comparison between the emission levels of numerical and experimental pollutants was discarded, as the difference in behavior between the temperature profiles shows that this first modeling does not satisfactorily represent the chemical/turbulent interactions of the flow under study, also affecting the concentration of species in the process exhaust gases.

The temperature profiles obtained in the numerical simulation by the FRED combustion modeling vary between 800 and 1000 °C, with values very close to the experimental ones that were also present in this range. The difference between temperature values is between 1.0 and 12.5%. The value of 12.5% refers to a measurement point that is located in the vicinity of the chamber wall and can be related to the radiation modeling in that region. However, this value did not significantly affect the numerical temperature profile of the combustion atmosphere.

The levels of UHC, CO and NO emissions obtained in the numerical simulations by FRED modeling also showed good agreement with the experimental values. The maximum deviation between the numerical and experimental values is of the order of 6%, which shows that the chosen numerical models and the reaction mechanism of the ethanol used adequately represent the combustion reactions that are developed in the process under study.

The validation of the combustion modeling was performed considering a numerical simulation time of 550 advances and the physical and thermodynamic characteristics of the combustion atmosphere showed that during the experiment the flameless combustion regime was not achieved. What was observed is that the system operated in the transition between the conventional combustion regime and the flameless combustion regime, which was evidenced by the presence of flame in the combustion atmosphere and asymmetric distribution of temperatures in the

combustion atmosphere, although the values of temperature had low gradients between the measurement points in the chamber. However, once the numerical procedure developed in the present work was validated, a new numerical analysis was performed considering a numerical simulation time of 1000 advances, which reinforced the previous conclusion. The analysis of the combustion atmosphere for 1000 numerical advances in time showed a homogeneous and practically symmetrical temperature distribution in the combustion atmosphere, better recirculation of the mixture between the reactants and hot gases resulting from combustion, a decrease of approximately 10% in the emission levels of pollutants, when compared to the simulation of 550 numerical advances in time, and, although there is no significant difference in temperature values for the two simulations, the temperature gradients remained around 230 °C. This set of physical and thermodynamic characteristics obtained in the simulation with 1000 numerical advances in time showed the development of the combustion regime with no visible flame, showing that the experimental procedure must be optimized from the point of view of the chamber's operating time so that the experimental results consistent with the flameless combustion regime.

Finally, the numerical procedure developed in the present work proved to be very satisfactory for the analysis of combustion systems operating in the flameless regime for burning liquid biofuels, highlighting important concepts that must be taken into account to carry out improvements in experiments involving the problem addressed in this study. This procedure will be extremely important for further studies in the system under analysis into this paper, allowing the optimization of the geometry of the combustion chamber, the fuel injection system, the operating time of the combustion system and the use of new liquid biofuels for analysis of the combustor performance.

ACKNOWLEDGEMENTS

The authors are grateful to CAPES, FAPEMIG and CNPq for financial help and ESSS for technical support which contributed to the development of this work.

NOMENCLATURES

K	Turbulent kinetic energy
V	Velocity (m/s)
$\dot{m}$	Mass flow rate (g/s)
T	Temperature (°C)

GREEK SYMBOLS

ε	Turbulent dissipation
λ	Excess air coefficient
Δ	Gradient

ABREVIATIONS

EDC	Eddy Dissipation Concept
FRED	Finite Rate Eddy Dissipation
CFD	Computational Fluid Dynamics
FRCM	Finite Rate Chemistry Model
RSM	Reynolds Stress Model
FGM	Flamelet Generated Manifold
OH	Hydroxyl radical
UHC	Unburned Hydrocarbon
RNG	Re-Normalisation Group
FRCM	Finite Rate Chemistry Model
DPM	Discret Phase Model
CAPES	Coordenação de Aperfeiçoamento de Pessoal de Nível Superior
CNPq	Conselho Nacional de Desenvolvimento Científico e Tecnológico
FAPEMIG	Fundação de Amparo à Pesquisa do Estado de Minas Gerais
ESSS	Engineering Simulation and Scientific Software

REFERENCES

[1] J.A. Wünning, J.G. Wünning, Flameless oxidation to reduce thermal no-formation, Prog. Energy Combust. Sci. 23 (1997) 81–94. https://doi.org/10.1016/s0360-1285(97)00006-3.

[2] F. Xing, A. Kumar, Y. Huang, S. Chan, C. Ruan, S. Gu, X. Fan, Flameless combustion with liquid fuel: A review focusing on fundamentals and gas turbine application, Appl. Energy. 193 (2017) 28–51. https://doi.org/10.1016/j.apenergy.2017.02.010.

[3] M. Derudi, R. Rota, Experimental study of the mild combustion of liquid hydrocarbons, Proc. Combust. Inst. 33 (2011) 3325–3332. https://doi.org/10.1016/j.proci.2010.06.120.

[4] C.G. de Azevedo, J.C. de Andrade, F. de Souza Costa, Flameless compact combustion system for burning hydrous ethanol, Energy. 89 (2015) 158–167. https://doi.org/10.1016/j.energy.2015.07.049.

[5] V.K. Arghode, A.K. Gupta, Effect of flow field for colorless distributed combustion (CDC) for gas turbine combustion, Appl. Energy. 87 (2010) 1631–1640. https://doi.org/10.1016/j.apenergy.2009.09.032.

[6] M. Castela, A.S. Veríssimo, A.M.A. Rocha, M. Costa, Experimental study of the combustion regimes occurring in a laboratory combustor, Combust. Sci. Technol. 184 (2012) 243–258. https://doi.org/10.1080/00102202.2011.630592.

[7] A. Cavaliere, M. De Joannon, Mild combustion, 2004. https://doi.org/10.1016/j.pecs.2004.02.003.

[8] A.K. Gupta, Flame characteristics with high temperature air combustion, in: 38th Aerosp. Sci. Meet. Exhib. 2000. https://doi.org/10.2514/6.2000-593.

[9] M. Ayoub, C. Rottier, S. Carpentier, C. Villermaux, A.M. Boukhalfa, D. Honoré, An experimental study of mild flameless combustion of methane/hydrogen mixtures, Int. J. Hydrogen Energy. 37 (2012) 6912–6921. https://doi.org/10.1016/j.ijhydene.2012.01.018.

[10] A.A.A. Abuelnuor, M.A. Wahid, A. Saat, M. Osman, Characterization of a Low NO x

Flameless Combustion Burner Using Natural Gas, J. Teknol. 2 (2014) 121–125.

[11] S.E. Hosseini, M.A. Wahid, S. Salehirad, Environmental protection and fuel consumption reduction by flameless combustion technology: A review, Appl. Mech. Mater. 388 (2013) 292–297. https://doi.org/10.4028/www.scientific.net/AMM.388.292.

[12] C.G. de Azevedo, Development of a compact flameless combustion system using a blurry injector for burning biofuels, Instituto Nacional de Pesquisas Espaciais, 2013.

[13] A.H. Lefebvre, Dilip R. Ballal, Gas Turbine Combustion, 3rd ed., CRC Press, Boca Raton, 2010. https://doi.org/https://doi.org/10.1201/9781420086058.

[14] M.C. Cameretti, R. Plazzesi, F. Reale, R. Tuccillo, CFD analysis of the flameless combustion in a micro-gas turbine, in: Proc. ASME Turbo Expo, Orlando, Flórida, USA, 2009: pp. 275–285. https://doi.org/10.1115/GT2009-59750.

[15] W. Yang, W. Blasiak, Mathematical modelling of NO emissions from high-temperature air combustion with nitrous oxide mechanism, Fuel Process. Technol. 86 (2005) 943–957. https://doi.org/10.1016/j.fuproc.2004.10.005.

[16] M. Torresi, S.M. Camporeale, B. Fortunato, S. Ranaldo, M. Mincuzzi, Diluted combustion in a aerodynamically staged swirled burner fueled by diesel oil, in: Process. Technol. a Sustain. Energy, 2010: pp. 1–8. https://doi.org/10.4405/ptse2010.I11.

[17] S. H. JAMALI, Computational Modeling of Turbulent Ethanol Spray Flames in a Hot Diluted Coflow, Delft University of Technology, 2015.

[18] J. Aminian, C. Galletti, S. Shahhosseini, L. Tognotti, Numerical investigation of a MILD combustion burner: Analysis of mixing field, chemical kinetics and turbulence-chemistry interaction, Flow, Turbul. Combust. 88 (2012) 597–623. https://doi.org/10.1007/s10494-012-9386-z.

[19] M. Bösenhofer, E.M. Wartha, C. Jordan, M. Harasek, The eddy dissipation concept-analysis of different fine structure treatments for classical combustion, Energies. 11 (2018) 1–21. https://doi.org/10.3390/en11071902.

[20] R. Weber, J.P. Smart, W. Vd Kamp, On the (MILD) combustion of gaseous, liquid, and solid fuels in high temperature preheated air, Proc. Combust. Inst. 30 II (2005) 2623–2629. https://doi.org/10.1016/j.proci.2004.08.101.

[21] T. Poinsont, D. Veynant, Theoretical and Numerical Combustion, 2nd ed., R.T. Edwards, Philadelphia, PA, USA, 2005.

[22] R.S. Cant, E. Mastorakos, An Introduction to Turbulent Reacting Flows, Imperial College Press, London, UK, 2008. https://doi.org/https://doi.org/10.1142/p498.

[23] S.S. Verma, Low temperature oxidation of ethanol, Indian J. Chem. Technol. 11 (2004) 410–422.

[24] B.E. Launder, D.B. Spalding, The numerical computation of turbulent flows, Comput. Methods Appl. Mech. Eng. 3 (1974) 269–289. https://doi.org/https://doi.org/10.1016/0045-7825(74)90029-2.

[25] B.O.P. e S. Siqueira, Numerical Simulation of the Flameless Combustion Regime Applied to the Burning of Hydrous Ethanol, Federal University of Itajubá, 2016. https://repositorio.unifei.edu.br/xmlui/handle/123456789/1233.

[26] D. Toporov, Combustion of Pulverised Coal in a Mixture of Oxygen and Recycled Flue Gas, 1st ed., Elsevier Ltd, 2015. https://doi.org/10.1016/C2013-0-19301-4.

[27] Z. Chen, J. Wen, B. Xu, S. Dembele, Large eddy simulation of fire dynamics with the improved eddy dissipation concept, Fire Saf. Sci. (2011) 795–808. https://doi.org/10.3801/IAFSS.FSS.10-795.

[28] F.C. Lockwood, N.G. Shah, A new radiation solution method for incorporation in general combustion procedures, in: Eighteenth Symp. Int. Combust., 1981: pp. 1405–1414. https://doi.org/https://doi.org/10.1016/S0082-0784(81)80144-0.

[29] W. A. Sirigano, Fluid Dynamics and Transport of Droplets and Sprays, Cambridge University Press, 1999. https://doi.org/https://doi.org/10.1017/CBO9780511529566.

[30] Gutheil E. (2011) Issues in Computational Studies of Turbulent Spray Combustion. In: Merci B., Roekaerts D., Sadiki A. (eds) Experiments and Numerical Simulations of Diluted Spray Turbulent Combustion. ERCOFTAC Series, vol 17. Springer, Dordrecht. https://doi.org/10.1007/978-94-007-1409-0_1.

[31] D. Rochaya, Numerical simulation of spray combustion using bio-mass derived liquid fuels, Cranfield University, 2007. http://hdl.handle.net/1826/2231.

[32] C. Bekdemir, Numerical Modeling of Diesel Spray Formation and Combustion, Eindhoven University of Technology, 2008.

[33] S. Kumar, P.J. Paul, H.S. Mukunda, Investigations of the scaling criteria for a mild combustion burner, Proc. Combust. Inst. 30 II (2005) 2613–2621. https://doi.org/10.1016/j.proci.2004.07.045.

[34] M. Mancini, R. Weber, U. Bollettini, Predicting NOx emissions of a burner operated in flameless oxidation mode, Proc. Combust. Inst. 29 (2002) 1155–1163. https://doi.org/10.1016/s1540-7489(02)80146-8.